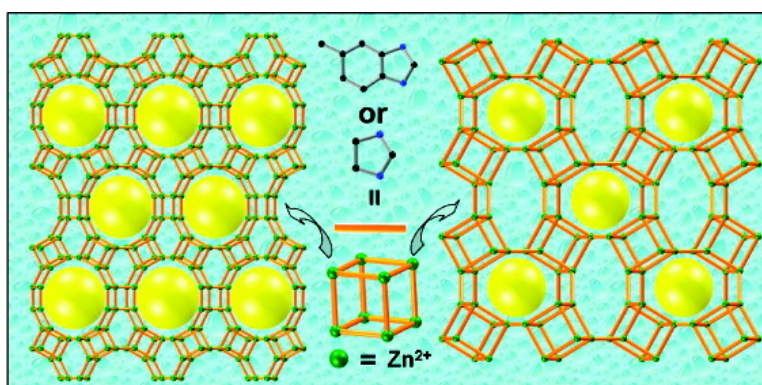Article

New Zeolitic Imidazolate Frameworks: From Unprecedented Assembly of Cubic Clusters to Ordered Cooperative Organization of Complementary Ligands

Tao Wu, Xianhui Bu, Jian Zhang, and Pingyun Feng

More About This Article

Additional resources and features associated with this article are available within the HTML version:

- Supporting Information
- Access to high resolution figures
- Links to articles and content related to this article
- Copyright permission to reproduce figures and/or text from this article

View the Full Text HTML

Articles

New Zeolitic Imidazolate Frameworks: From Unprecedented Assembly of Cubic Clusters to Ordered Cooperative Organization of Complementary Ligands

Tao Wu,[†] Xianhui Bu,[‡] Jian Zhang,[‡] and Pingyun Feng*,[†]

Department of Chemistry, University of California, Riverside, California 92521, and Department of Chemistry and Biochemistry, California State University, 1250 Bellflower Boulevard, Long Beach, California 90840

Five 4-connected zeolitic metal imidazolate frameworks have been synthesized by using complementary ligands in combination with fine-tuning of synthetic parameters such as solvent ratio. These materials exhibit four different tetrahedral topologies. In **TIF-2** and **TIF-3**, the cubic double 4-ring units are assembled into two different topologies not previously found in metal imidazolates. **TIF-2** possesses one-dimensional 12-ring channels and an unprecedented 4-connected topology. It exhibits permanent microporosity and high thermal stability. **TIF-3** is the first known example of metal imidazolates with the zeolitic ACO topology. In **TIF-4**, **TIF-5Zn**, and **TIF-5Co**, two complementary ligands (one small and one large) control the framework topology in a cooperative manner with small ligands favoring small rings (such as 4-rings) and large ligands favoring large rings such as 6- and 8-rings, which highlights the significance of framework building units (i.e., cross-linking ligands) in the control of the framework topology, in distinct contrast with inorganic framework materials (e.g., zeolites) in which the framework topology is primarily controlled by extra-framework structure-directing agents. These new frameworks underline the rich synthetic and structural chemistry of metal-imidazolate-based porous frameworks.

Introduction

As two important families of crystalline microporous materials, porous inorganic framework materials (e.g., zeolites) and metal-organic frameworks (MOFs) have attracted much attention because of their applications in gas adsorption, separation, catalysis, and so forth.[1–9] In recent years, in order to combine their respective advantages, an increasing interest has been directed at synthetic development of metal-organic frameworks with topological features characteristic

of those in 4-connected zeolites.[10–15] Among various efforts to extend zeolite framework types in MOFs and to tune their compositional and topological features, the exploration of tetrahedral imidazolate frameworks has been particularly

* Corresponding author. E-mail: pingyun.feng@ucr.edu.
† University of California.
‡ California State University.

(1) (a) Breck, D. W. *Zeolite Molecular Sieves*; Wiley: New York, 1974. (b) Maesen, T. L. M.; Marcus, B. *Introduction to Zeolite Science and Practice*; Elsevier: Amsterdam, 2001; pp 1–9. (c) Van Bekkum, H.; Flanigen, E. M.; Jacobs, P. A.; Jansen, J. C. *Introduction to Zeolite Science and Practice*; Elsevier, Amsterdam, 2001. (d) Bu, X.; Feng, P.; Stucky, G. D. *Science* **1997,** *278,* 2080–2085. (e) Davis, M. E. *Nature* **2002,** *417,* 813–821.

(2) (a) Xing, H. Z.; Li, J. Y.; Yan, W. F.; Chen, P.; Jin, Z.; Yu, J. H.; Dai, S.; Xu, R. R. *Chem. Mater.* **2008,** *20,* 4179–4181. (b) Li, Y.; Yu, J. H.; Xu, R. R.; Baerlocher, C.; McCusker, L. B. *Angew. Chem., Int. Ed.* **2008,** *47,* 4401–4405. (c) Zhao, L.; Li, J. Y.; Chen, P.; Li, G. H.; Yu, J. H.; Xu, R. R. *Chem. Mater.* **2008,** *20,* 17–19.

(3) (a) de Lill, D. T.; Cahill, C. L. *Cryst. Growth Des.* **2007,** *7,* 2390–2393. (b) Knope, K. E.; Cahill, C. L. *Inorg. Chem.* **2007,** *46,* 6607–6612. (c) de Lill, D. T.; Cahill, C. L. *Chem. Commun.* **2006,** 4946–4948.

(4) (a) Oliver, S.; Kuperman, A.; Ozin, G. A. *Angew. Chem., Int. Ed.* **1998,** *37,* 46–62. (b) Oliver, S.; Kuperman, A.; Lough, A.; Ozin, G. A. *Chem. Mater.* **1996,** *8,* 2391–2398.

(5) (a) Christensen, K. E.; Bonneau, C.; Gustafsson, M.; Shi, L.; Sun, J. L.; Grins, J.; Jansson, K.; Sbille, I.; Su, B. L.; Zou, X. D. *J. Am. Chem. Soc.* **2008,** *130,* 3758–3759. (b) Christensen, K. E.; Shi, L.; Conradsson, T.; Ren, T. Z.; Dadachov, M. S.; Zou, X. D. *J. Am. Chem. Soc.* **2006,** *128,* 14238–14239. (c) Zou, X. D.; Conradsson, T.; Klingstedt, M.; Dadachov, M. S.; O'Keeffe, M. *Nature* **2005,** *437,* 716–719.

(6) (a) Pan, C. Y.; Liu, G. Z.; Zheng, S. T.; Yang, G. Y. *Chem. Eur. J.* **2008,** *14,* 5057–5063. (b) Zheng, S. T.; Zhang, J.; Yang, G. Y. *Angew. Chem., Int. Ed.* **2008,** *47,* 3909–3913. (c) Liu, G. Z.; Zheng, S. T.; Yang, G. Y. *Angew. Chem., Int. Ed.* **2007,** *46,* 2827–2830.

(7) (a) Chen, B. L.; Wang, L. B.; Zapata, F.; Qian, G. D.; Lobkovsky, E. B. *J. Am. Chem. Soc.* **2008,** *130,* 6718–6719. (b) Chen, B. L; Yang, Y.; Zapata, F.; Lin, G. N.; Qian, G. D.; Lobkovsky, E. B. *Adv. Mater.* **2007,** *19,* 1693–1696.

(8) (a) Férey, G.; Mellot-Draznieks, C.; Serre, C.; Millange, F. *Acc. Chem. Res.* **2005,** *38,* 217–225. (b) Yaghi, O. M.; O'Keeffe, M.; Ockwig, N. W.; Chae, H.; Eddaoudi, M.; Kim, J. *Nature* **2003,** *423,* 705–714. (c) Liu, Y.; Eubank, J. F.; Cairns, A. J.; Eckert, J.; Kravtsov, V. C.; Luebke, R.; Eddaoudi, M. *Angew. Chem., Int. Ed.* **2007,** *46,* 3278–3283. (d) Mulfort, K. L.; Hupp, J. T. *J. Am. Chem. Soc.* **2007,** *129,* 9604–9605. (e) Dinca, M.; Yu, A. F.; Long, J. R. *J. Am. Chem. Soc.* **2006,** *128,* 8904–8913. (f) Evans, O. R.; Lin, W. *Acc. Chem. Res.* **2002,** *35,* 511–512. (g) Lin, X.; Blake, A. J.; Wilson, C.; Sun, X. Z.; Champness, N. R.; George, M. W.; Hubberstey, P.; Mokaya, R.; Schröder, M. *J. Am. Chem. Soc.* **2006,** *128,* 10745–10753. (h) Lee, E. Y.; Suh, M. P. *Angew. Chem., Int. Ed.* **2004,** *43,* 2798–2801. (i) Kitagawa, S.; Kitaura, R.; Noro, I. S. *Angew. Chem., Int. Ed.* **2004,** *43,* 2334–2375.

successful.[11−15] In 4-connected imidazolate frameworks, divalent metal ions (such as Zn^{2+}, Co^{2+}) replace T atoms (tetrahedral atoms such as Si, Al, P), and imidazolates ($Im^−$) substitute for bridging $O^{2−}$ in zeolites, resulting in a number of 4-connected frameworks with the general framework composition of $M(im)_2$ and topological types such as ANA (analcime), BCT, DFT, GIS (gismondine), GME (gmelinite), LTA, MER (merlinoite), RHO, and SOD (sodalite).

In the synthesis of zeolites, extra-framework structure directing agents (e.g., tetraalkylammonium cations) play an important role in determining the framework topology. The structural diversity of zeolites is in a large part due to the effect of various structural directing agents. In metal imidazolates, while the structure directing effect of extra-framework species (usually solvents) may still be used to promote the crystallization and control the product topology, another important factor, the type of imidazolate ligand, has become a focus in the research into creating novel zeolitic topologies. In addition to the ligand−solvent interaction, the ligand−ligand interaction in metal imidazolates has been recognized as a variable that can be utilized to control the framework topology.[14b] Such ligand−ligand interactions can be tuned by the type, number, and position of substituents

Scheme 1. Schematic Display of the Relative Orientation of Imidazolate Rings[a] (top) and Schematic Display of the Relative Position of Adjacent 8 Nodes[b] (bottom)
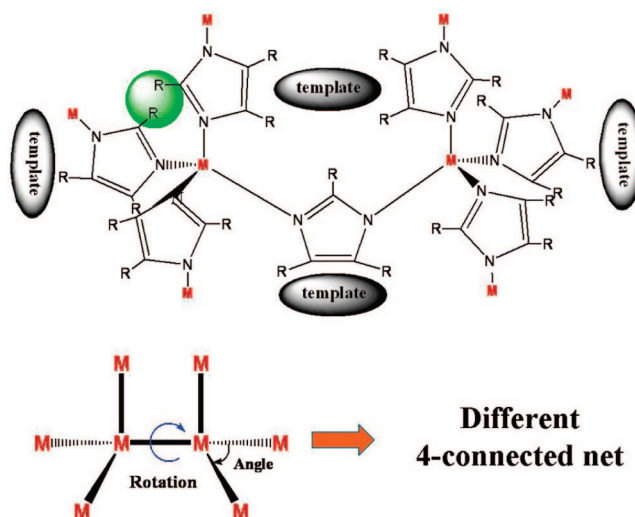
[a] This is strongly affected by the steric hindrance of substituted groups, size of template molecules, and the interactions between the substituted groups and template molecules. [b] Such as M−M−M angle and M−M−M−M torsion angle tuned by different orientation of imidaozlate, which induce the different zeolitic topology and porosity.

on the imidazolate ring. They can also be tuned by using two or more complementary imidazolate ligands in the same assembly process. So an in-depth understanding of ligands' orientation and ligand−ligand interactions is vital for rational construction of novel zeolitic imidazolate frameworks (Scheme 1). One obstacle to the understanding of the role of ligand is the possible orientational disorder of the imidazolate ligand in a porous framework. Such a tendency to be disordered should be stronger when two different ligands are coassembled into the same framework, particularly if the two ligands used do not differ significantly.

Here, we report five zeolitic structures (denoted as TIF-*n*, TIF = tetrahedral imidazolate framework, *n* = 2−5) prepared by using the mixed-ligand synthetic strategy. These five structures exhibit four types of 4-connected topology and are synthesized through the selection of two complementary ligands: one small-sized imidazole ligand with no substituent groups and one large-sized ligand with a relatively large substituent group (5-methylbenzimidazole, or 5,6-dimethylbenzimidazole). An attractive feature of TIF-2 and TIF-3 is its cubic structural building unit (also called double four-ring units, d4R) which is well-known because of its presence in the industrially important zeolite A. However, the organization of d4R units in TIF-2 and TIF-3 is totally different from that in zeolite A. TIF-2 has an unprecedented 4-connected topology and features one-dimensional large pore channels (i.e., the pore window with 12 tetrahedral vertices). TIF-3 possesses the distorted body-centered cubic (bcc) arrangement of d4R units and its topological type (ACO) has not been previously found in metal imidazolates. TIF-4 and TIF-5 also have 4-connected tetrahedral frameworks, and they are of particular interest because the strict ordering of two complementary ligands in their frameworks

(9) (a) Férey, G. *Chem. Soc. Rev.* **2008**, *37*, 191–214. (b) Kitagawa, S.; Matsuda, R. *Coord. Chem. Rev.* **2007**, *251*, 2490–2509. (c) Matsuda, R.; Kitaura, R.; Kitagawa, S.; Kubota, Y.; Belosludov, R. V.; Kobayashi, T. C.; Sakamoto, H.; Chiba, T.; Takata, M.; Kawazoe, Y.; Mita, Y. *Nature* **2005**, *436*, 238–241. (d) Kepert, C. J. *Chem. Commun.* **2006**, 696–700. (e) Fletcher, A. J.; Thomas, K. M.; Rosseinsky, M. J. *J. Solid State Chem.* **2005**, *178*, 2491–2510. (f) Kitagawa, S.; Uemura, K. *Chem. Soc. Rev.* **2005**, *34*, 109–119. (g) Bradshaw, D.; Claridhe, J. B.; Cussen, E. J.; Prior, T. J.; Rosseinsky, M. J. *Acc. Chem. Res.* **2005**, *38*, 273–282. (h) Ghosh, S. K.; Zhang, J. P.; Kitagawa, S. *Angew. Chem., Int. Ed.* **2007**, *46*, 7965–7968. (i) Serre, C.; Mellot-Draznieks, C.; Surble, S.; Audebrand, N.; Filinchuk, Y.; Férey, G. *Science* **2007**, *315*, 1828–1831. (j) Papaefstathiou, G. S.; MacGillivary, L. R. *Coord. Chem. Rev.* **2003**, *246*, 169–184. (k) Lee, Y. E.; Jang, S. Y.; Suh, M. P. *J. Am. Chem. Soc.* **2005**, *127*, 6374–6381. (l) Matsuda, R.; Kitaura, R.; Kitagawa, S.; Kubota, Y.; Kobayashi, T. C.; Horike, S.; Takata, M. *J. Am. Chem. Soc.* **2004**, *126*, 14063–14070.

(10) (a) Férey, G.; Serre, C.; Millange, F.; Surble, S.; Dutour, J.; Margiolaki, I. *Angew. Chem., Int. Ed.* **2004**, *43*, 6296–6301. (b) Fang, Q.; Zhu, G.; Xue, M.; Sun, J.; Wei, Y.; Qiu, S. L.; Xu, R. R. *Angew. Chem., Int. Ed.* **2005**, *44*, 3845–3848. (c) Navarro, J. A. R.; Barea, E.; Salas, J. M.; Masciocchi, N.; Galli, S.; Sironi, A.; Ania, C. O.; Parra, J. B. *Inorg. Chem.* **2006**, *45*, 2397–2399. (d) Guo, X. D.; Zhu, G. S.; Li, Z. Y.; Chen, Y.; Li, X. T.; Qiu, S. L. *Inorg. Chem.* **2006**, *45*, 4065–4070. (e) Liu, Y.; Kravtsov, V. C.; Larsen, R.; Eddaoudi, M. *Chem. Commun.* **2006**, 1488–1490. (f) Sava, D. F.; Kravtsov, V. C.; Nouar, F.; Wojtas, L.; Eubank, J. F.; Eddaoudi, M. *J. Am. Chem. Soc.* **2008**, *130*, 3768–3770.

(11) (a) Tian, Y. Q.; Cai, C. X.; Ji, Y.; You, X. Z.; Peng, S. M.; Lee, G. S. *Angew. Chem., Int. Ed.* **2002**, *41*, 1384–1386. (b) Tian, Y. Q.; Cai, C. X.; Ren, X. M.; Duan, C. Y.; Xu, Y.; Gao, S.; You, X. Z. *Chem. Eur. J.* **2003**, *9*, 5673–5685. (c) Tian, Y.-Q.; Chen, Z. X.; Weng, L.-H.; Guo, H. B.; Gao, S.; Zhao, D. Y. *Inorg. Chem.* **2004**, *43*, 4631–4635. (d) Tian, Y.-Q.; Xu, L.; Cai, C.-X.; Wei, J.-C.; Li, Y.-Z.; You, X. Z. *Eur. J. Inorg. Chem.* **2004**, 1039–1044.

(12) Tian, Y.-Q.; Zhao, Y.-M.; Chen, Z.-X.; Zhang, G.-N.; Weng, L.-H.; Zhao, D.-Y. *Chem. Eur. J.* **2007**, *13*, 4146–4154.

(13) (a) Huang, X.-C.; Lin, Y.-Y.; Zhang, J. P.; Chen, X.-M. *Angew. Chem., Int. Ed.* **2006**, *45*, 1557–1559. (b) Huang, X.-C.; Zhang, J.-P.; Chen, X.-M. *Chin. Sci. Bull.* **2003**, *48*, 1531–1534.

(14) (a) Park, K. S.; Ni, Z.; Côté, A. P.; Choi, J. Y.; Huang, R.; Uribe-Romo, F. J.; Chae, H. K.; O'Keeffe, M.; Yaghi, O. M. *Proc. Natl Acad. Sci. U.S.A.* **2006**, *103*, 10186–10191. (b) Hayashi, H.; Côté, A. P.; Furukawa, H.; O'Keeffe, M.; Yaghi, O. M. *Nat. Mater.* **2007**, *6*, 501–506.

(15) (a) Banerjee, R.; Phan, A.; Wang, B.; Knobler, C.; Furukawa, H.; O'keeffe, M.; Yaghi, O. M. *Science* **2008**, *319*, 939–943. (b) Wang, B.; Côté, A. P.; Furukawa, H.; O'Keeffe, M.; Yaghi, O. M. *Nature* **2008**, *453*, 207–211.

Table 1. Crystallographic and Structure Refinement Parameters for TIF-*n*

	TIF-2 $[Zn(Im)_{1.10}(MBim)_{0.90}]\cdot$ $\sim 2.5(C_6H_6)$	TIF-3 $[Zn(Im)_x(MBim)_y]\cdot$ $(G)_z$ $(x + y = 2)$	TIF-4 $[Zn(Im)_{1.5}(MBim)_{0.5}]\cdot$ $0.5(C_6H_6)$	TIF-5Zn $[Zn(Im)(DMBim)]\cdot$ $\sim 1.5H_2O$	TIF-5Co $[Co(Im)(DMBim)]\cdot$ $\sim 1.5H_2O$
formula	$C_{25.5}H_{24.6}N_4Zn$	$C_{9.13}H_{10}N_4Zn$	$C_{11.50}H_{11}N_4Zn$	$C_{12}H_{15}N_4O_{1.5}Zn$	$C_{12}H_{15}N_4O_{1.5}Co$
formula weight	452.48	241.15	270.63	304.66	325.23
crystal system	orthorhombic	monoclinic	orthorhombic	tetragonal	tetragonal
space group	*Pnma*	*C*2/*c*	*Pbca*	*I*4$_1$/*a*	*I*4$_1$/*a*
a, Å	17.6356(5)	25.9164(10)	15.6251(9)	16.7862(2)	16.6286(2)
b, Å	48.0644(13)	24.8826(10)	16.3217(9)	16.7862(2)	16.6286(2)
c, Å	24.5539(7)	17.9542(6)	18.1244(10)	21.3384(5)	21.4148(4)
α, deg	90	90	90	90	90
β, deg	90	93.206(3)	90	90	90
γ, deg	90	90	90	90	90
V, Å^3	20813.0(10)	11560.0(8)	4622.2(4)	6012.66(17)	5921.41(15)
Z	48	32	16	16	16
d_{calcd}, g·cm^{-3}	1.004	1.062	1.555	1.306	1.298
μ, mm^{-1}	1.399	1.673	2.104	1.628	1.153
GOF	1.076	1.019	1.091	1.175	1.077
R_1	0.0955	0.1270	0.0709	0.0938	0.0652
wR_2 (all data)	0.2742	0.3615	0.2448	0.2959	0.2156
topology		ACO	cag	GIS	GIS

provides a unique opportunity for probing their synergistic effect in the self-assembly process.

Experimental Section

Materials and Methods. All reagents and solvents employed were commercially available and used as supplied without further purification. TGA was carried out on a TA SDT Q600 thermal analysis system. Powder X-ray diffraction data were collected using a Bruker D8 Advance powder diffractometer operating at 40 kV and 40 mA for Cu Kα radiation (λ = 1.5406 Å).

Synthesis of TIF-2. Zn(Ac)$_2$·2H$_2$O (117.8 mg, 0.5367mmol), 5-methylbenzimidazole (70.3 mg, 0.5320mmol), imidazole (44.2 mg, 0.6492mmol), ($\pm$)-2-amino-1-butanol (4.0 mL), and benzene (3.6 mL) are mixed in a Teflon-lined autoclave and stirred for 0.5 h. The autoclave was then sealed and heated up at 150 °C for 5 days, followed by cooling down to room temperature. A large amount of small colorless crystalline materials were obtained with a yield of 35.4% (based on zinc salt). The crystals were washed using ethanol three times and dried in air for other measurements. Elemental analysis of as-synthesized sample: C, 49.22; H, 4.02; N, 20.98. Elemental analysis of sample dried at 300 °C: C, 47.93; H, 3.78; N, 20.78.

Synthesis of TIF-3. Zn(Ac)$_2$·2H$_2$O (116.2 mg, 0.5294 mmol), 5-methylbenzimidazole (71.2 mg, 0.5387 mmol), imidazole (41.7 mg, 0.6125 mmol), ($\pm$)-2-amino-1-butanol (4.0 mL) and benzene (0.4 mL) are mixed in a Teflon-lined autoclave and stirred for 0.5 h. The autoclave was then sealed and heated up at 150 °C for 6 days, followed by cooling to room temperature. Small colorless crystals were obtained as a minor phase, accompanied with a large amount of unidentified polycrystalline powder.

Synthesis of TIF-4. Zn(Ac)$_2$·2H$_2$O (114.5 mg, 0.5216 mmol), 5-methylbenzimidazole (26.9 mg, 0.2035 mmol), imidazole (57.6 mg, 0.8461 mmol), 3-amino-1-propanol (4.0 mL) and benzene(2.0 mL) are mixed in a Teflon-lined autoclave and stirred for 0.5 h. The autoclave was then sealed and heated up at 150 °C for 5 days, followed by cooling to room temperature. A large amount of colorless octahedral crystalline materials was obtained with a yield of 42.3% (based on zinc salt). The crystals were washed using ethanol three times and dried in air for other measurements.

Synthesis of TIF-5Zn. Zn(Ac)$_2$·2H$_2$O (122.7 mg, 0.5590 mmol), 5,6-dimethylbenzimidazole (77.2 mg, 0.5281 mmol), imidazole (60.7 mg, 0.8916), ($\pm$)-2-amino-1-butanol (3.0 mL), and *p*-xylene (1.0 mL) are mixed in a Teflon-lined autoclave and stirred for 0.5 h. The autoclave was then sealed and heated up at 150 °C for 5 days,

followed by cooling to room temperature. A large amount of colorless crystalline materials was obtained with a yield of 35.5% (based on zinc salt). The crystals were washed using ethanol three times and dried in air for other measurements.

Synthesis of TIF-5Co. Co(Ac)$_2$·4H$_2$O (128.2 mg, 0.5147 mmol), 5,6-dimethylbenzimidazole (80.2 mg, 0.5486 mmol), imidazole (50.9 mg, 0.7476 mmol), and 3-amino-1-propanol (6.0 mL) are mixed in a Teflon-lined autoclave and stirred for 0.5 h. The autoclave was then sealed and heated up at 150 °C for 5 days, followed by cooling to room temperature. A large amount of violet crystalline materials was obtained with a yield of 44.3% (based on cobalt salt). The crystals were washed using ethanol three times and dried in air for other measurements.

Single-Crystal X-ray Crystallography. Crystallographic data for single-crystal X-ray analysis were collected on a Bruker Smart APEX II CCD area diffractometer with nitrogen-flow temperature controller using graphite-monochromated Mo Kα radiation (λ = 0.71073 Å), operating in the ω and φ scan mode. The SADABS program was used for absorption correction. The structure was solved by direct methods, and the structure refinements were based on $|F^2|$.[16] Most of non-hydrogen atoms were refined with anisotropic displacement parameters, except the atoms of disordered fragments, which were refined isotropically. Hydrogen atoms were placed in calculated positions. All crystallographic calculations were conducted with the SHELXTL software suites. Solvent molecules and some imidazolate ligands are disordered, which contributes to the relatively high R-factors reported here.

Gas Adsorption Measurement. N$_2$ gas sorption experiments were carried out on a Micromeritics ASAP 2010 surface area and pore size analyzer. Prior to the measurement, the sample was treated using the following procedure. The as-synthesized sample of **TIF-2** was soaked with anhydrous methanol for 10 h, and the extract was discarded. The sample was then allowed to immerse in fresh methanol for about 15 h to remove benzene and water solvates. The similar immersion was utilized to treat the sample with dichloromethane to remove methanol solvates. After the removal of dichloromethane by centrifuging, the wet sample was dried under vacuum at ambient temperature for 20 h to yield an activated sample for gas adsorption measurements. Before the measurement, the sample was dried again by using the "degas" function of the surface area analyzer for 20 h at 250 °C. The N$_2$ adsorption measurement was performed at 77 K with liquid nitrogen.

(16) *Shelxtl 6.10*, Bruker Analytical Instrumentation: Madison, WI, 2000.
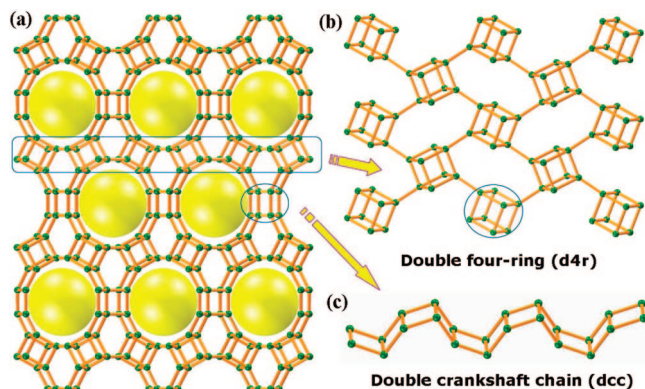
Figure 1. (a) Novel topology of **TIF-2** viewed along [001] direction; (b) 2-D layer viewed along [100], containing special double four-rings (*d4R*); (c) double crankshaft chain (*dcc*).

Results and Discussion

TIF-*n* were synthesized by solverthermal reactions of M(Ac)$_2$ (M = Zn^{2+} or Co^{2+}), imidazole, and 5-methylben-zimidazole (or 5,6-dimethylbenzimidazole) in mixed solvents (except for **TIF-5Co** which was made with only one solvent) at 150 °C. The crystal structures of **TIF-*n*** were determined by single-crystal X-ray diffraction (Table 1). They are stable in air and insoluble in water and common organic solvents.

Unprecedented Organization of *d4R* units in TIF-2. **TIF-2** crystallizes in an orthorhombic structure with space group *Pnma* and exhibits an unprecedented 4-connected zeolitic network. The asymmetric unit (Figure S1a, Support-ing Information) includes six zinc sites exhibiting three different secondary coordination environments in the ratio of 1:1:1 (T$_1$, T$_2$, and T$_3$; Figure S2, Supporting Information). All of these T atoms possess the same loop configuration. As in zeolites, each T atom is coordinated with four N atoms from four different ligands and each ligand links two T atoms. Unfortunately, due to the disorder of some atoms on the ligands, the ratio between two ligands cannot been determined by single-crystal X-ray diffraction. Elemental analysis gives a ratio of 0.9:1.1 between MBim and Im.

Of particular interest is the existence of double 4-rings in **TIF-2**. Being a basic secondary building unit (SBU), 4-rings lead to two basic composite building units: double 4-ring (*d4R*) and double crankshaft chain (*dcc*), as shown in Figure 1b,c, respectively. Each *dcc* consists of only T$_1$ atoms while each *d4R* is composed of four T$_2$ atoms and four T$_3$ atoms (Figure S3, Supporting Information). Figure 1b shows that each *d4R* is bonded to adjacent four *d4R* by T$_3$T$_3$ to form a 2-D layer parallel to (010) plane. Adjacent two 2-D layers are joined together by a set of *dcc* through T$_1$T$_2$ along the [001] direction to generate a 3-D framework (Figure 1a). Although *d4R* is an important composite building unit for the construction of some inorganic zeolite frameworks (such as ACO, −CLO, LTA, UFI, UTL),[17,18] it rarely occurs in metal-organic frameworks, and prior to this work, only two
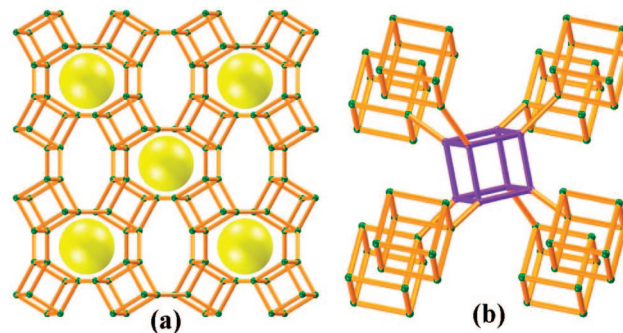

Figure 2. (a) ACO zeolite framework in **TIF-3** viewed along [001] direction; (b) each *d4R* is connected to 8 adjacent *d4R*.

examples of metal imidazolates containing *d4R* were reported. [14b,15b]

A striking feature of **TIF-2** is the presence of large 12-rings, which is confirmed by vertex symbols of T-atoms (4.6.4.10$_3$.4.10$_5$ for T$_1$; 4.4.4.6.4.10 for T$_2$; and 4.4.4.6.10.12 for T$_3$; Table S1, Supporting Information). The large 12-ring has a window size of 22.4 Å × 20.8 Å as measured using the zinc interatomic distances. So far, only a few metal imidazolate topologies contain large 12-rings, ZIFs with the GME,[15a] poz,[15b] and moz[15b] topologies and **TIF-1**.[19] **TIF-2** possesses a 3-D channel system with 1-D large pore 12-ring channel along the [001] direction, interconnected by 10-ring channels along the [100] direction (Figure 1a). The calculation using PLATON indicates that **TIF-2** has 41.5% of the total volume occupied by solvent molecules.[20]

TIF-2 has an unprecedented 4-connected zeolitic topology. The topology of **TIF-2** is different from another 1-D large-pore metal imidazolate with the GME topology because the composite building units in the GME topology is double 6-rings (*d6r*) and double crankshaft chains (*dcc*) (Figure S4, Supporting Information).

Organization of Cubic Double 4-Ring Units into 3-D Distorted Body-Centered Cubic Framework. By reducing the amount of cosolvent benzene and tuning the solvent ratio from 4: 3.6 to 4: 0.4 between (±)-2-amino-1- butanol and benzene, the organization of d4R units is dramatically altered, resulting in the formation of **TIF-3**. Similar to **TIF-2**, some atoms in bridging imidazolate ligands are disordered. How-ever, the topology of **TIF-3** can be reliably determined from the location of tetrahedral Zn^{2+} sites with the Zn···Zn distances ranging from 5.90 to 5.93 Å, which are typical in 4-connected zinc imidazolates. **TIF-3** possesses the uninodal ACO zeolite topology, which has only been found in an aluminum cobalt phosphate denoted as **ACP-1**.[21] Like **TIF-2**, *d4R* also exists in **TIF-3** as a composite building unit, and each *d4R* is joined to adjacent four *d4R* to form a 2-D layer parallel to the (100) plane. However, unlike **TIF-2**, in which neighboring two 2-D layers are joined by a set of *dcc*, all 2-D layers in **TIF-3** are directly joined with adjacent ones to give a 3-D framework (containing 1-D channels with an elliptical 8-rings opening) (Figure 2a). In general, each *d4R* can connect eight adjacent *d4R* to form an ideal ACO

(17) Baerlocher, C.; McCusker, L. B.; Olson, D. H. *Atlas of Zeolite Framework Types*, 6th ed.; Elsevier: Amsterdam, 2007.
(18) See database of Reticular Chemistry Structure Resource on the website: http://rcsr.anu.edu.au/.
(19) Wu, T.; Bu, X.; Liu, R.; Lin, Z. E.; Zhang, J.; Feng, P. *Chem. Eur. J.* **2008**, *14*, 7771–7773.
(20) Spek, A. L. *Acta Crystallogr., Sect. A* **1990**, *46*, C34.
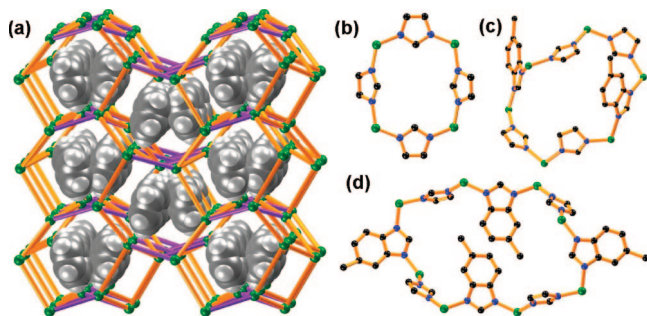(21) Feng, P.; Bu, X.; Stucky, G. D. *Nature* **1997**, *388*, 735–741.

Figure 3. (a) Cage topology of **TIF-4** viewed along [001] direction (the space filling is C_6H_6, green atom for Zn atom, orange bar for imidazolate, purple bar for 5-methylbenzimidazolate), containing $Zn_4(Im)_4$ four-ring (b), $Zn_6(Im)_4(5\text{-}MBim)_2$ six-ring (c), and $Zn_8(Im)_4(5\text{-}MBim)_4$ eight-ring (d).

Figure 4. (a) GIS Topology of **TIF-5** viewed along [100] (green atom for Zn^{2+} or Co^{2+}, orange bar for imidazolate, purple bar for 5,6-dimethylben-zimidazolate), containing $Zn_4(Im)_4$ four-ring (b), $Zn_4(Im)_2(5,6\text{-}DMBim)_2$ four-ring (c), and $Zn_8(Im)_2(5\text{-}MBim)_6$ eight-ring (d).

topology with space group $Im\bar{3}m$; however, the presence of organic ligands contributes to the observed lower symmetry (i.e., monoclinic) in **TIF-3** (Figure 2b).

Ordered Cooperative Assembly of Two Different Pairs of Complementary Ligands. By significantly increasing the ratio between imidazole and 5-methylbenzimidazole (from 1.2 to 4.2) and using a different solvent combination (3-amino-1-propanol and benzene, instead of (±)-2-amino-1-butanol and benzene for **TIF-2** and **TIF-3**), **TIF-4** with a topology totally different from **TIF-2** and **TIF-3** has been made. It crystallizes in orthorhombic space group *Pbca*, and each Zn ion is tetrahedrally coordinated to four nitrogen atoms from bridging imidazolates to furnish an infinite 3-D framework. Structural analysis reveals the exact positions and compositions of both types of ligands. The ratio of Im and MBim is 3:1, which reflects the high Im to MBim ratio in the starting synthetic mixture. **TIF-4** possesses a cag ($4^6 5$) topological net which can be regarded as adjacent $Zn_2(Im)_3$ layer with 4.8.8 sheet (Figure S5b, Supporting Information) connected by 5-methylbenzimidazolate (MBim) ligands. A view along the [010] direction shows 1-D channels with distorted hexagonal apertures, which are occupied by solvent benzene molecules (Figure 3a). The solvent-accessible volume of **TIF-4** is about 28.5%. An analysis of the structure shows that all four-rings are composed of the small-sized imidazolate ligands while six- and eight-rings contain both small-sized imidazolate ligands and the large-sized 5-meth-ylbenzimidazolate ligands, as shown in Figure 3b−d. Such a distribution of different-sized ligands illustrates the cooperative effects of these ligands in forming rings of various sizes, which ultimately controls the topological features of the resulting 3-D framework.

While **TIF-2**, **-3**, and **-4** were made with 5-methylbenz-imidazole as one of the framework building units, **TIF-5Zn** and **TIF-5Co** contain 5,6-dimethylbenzimidazole. **TIF-5Zn** crystallizes in a tetragonal space group $I4_1/a$. Structural analysis also reveals exact positions and compositions of two different ligands. The ratio of Im and DMBim is 1:1, as compared with the 3:1 ratio in **TIF-4**. **TIF-5Zn** possesses a GIS (gismondine) topological net constructed from basic composite building unit *dcc*. As shown in Figure S6 (Supporting Information), each *dcc* is formed by connecting $Zn_4(Im)_4$ rings with 5,6-dimethylbezimidazolate, and neigh-boring *dcc* chains are further joined together by 5,6-
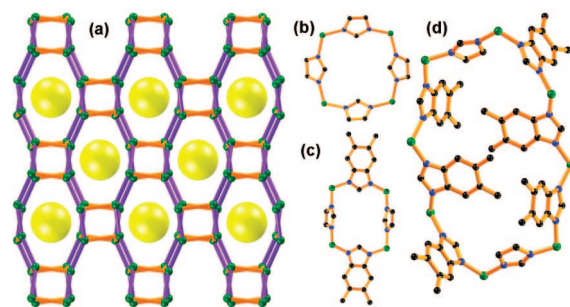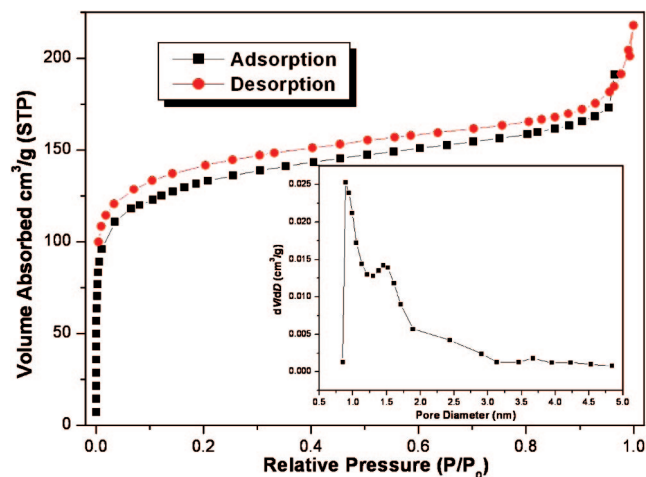

Figure 5. Nitrogen gas adsorption isotherm at 77K for **TIF-2**. P/P_0 is the ratio of gas pressure (P) to saturation pressure (P_0), with $P_0 = 740$ torr. Inset is the corresponding pore size distribution curves.

dimethylbenzimidazolate to give a 3-D framework. A view along the [100] direction reveals 1-D channels with distorted octagonal apertures, which are perpendicularly intersected by identical channels of 8-ring openings in the [010] direction (Figure 4a). In **TIF-5Zn**, half of four-rings are composed of $Zn_4(Im)_4$, and the second half of four-rings are made up of $Zn_4(Im)_2(DMBim)_2$. All 8-rings consist of two small-sized imidazolate ligands and six large-sized $DMBim^-$ ligands, two of which point inward to the center of eight-rings (Figure 4b−d). It is clear that the large-sized imidazolate ligands prefer large-sized rings. To prevent all the channel volume from being occupied by the substituents of these ligands, small-sized imidazolate ligands can be introduced into the large ring to tune the channel size. **TIF-5Co** is isostructural to **TIF-5Zn** except that Zn^{2+} is replaced by Co^{2+} in **TIF-5Co**. The solvent-accessible volume is approximately about 26.1%.

Properties of TIF-*n*. Despite the highly open framework topology, **TIF-2** exhibits very high thermal stability. Thermal gravimetric analysis (TGA) under the N_2 atmosphere performed on **TIF-2** (washed with ethanol and dried in air) shows a gradual weight loss of 4.3% between 30 and 200 °C, due to the loss of benzene solvent molecules. A long plateau in the temperature range between 200 and 480 °C was observed (Figure S7, Supporting Information). TGA of

TIF-4 shows loss of extra-framework benzene molecules below 284 °C (10.5%). There is no further weight lose in the temperature range of 284−478 °C (Figure S8, Supporting Information). **TIF-5Zn** exhibits a gradual weight loss of 9.3% below 386 °C, indicating the removal of water molecules (Figure S9, Supporting Information). The TG curve of **TIF-5Co** also gives a 9.7% of weight loss below 322 °C (Figure S10, Supporting Information).

The permanent porosity of **TIF-2** was confirmed by N_2 gas adsorption measurements performed on Micromeritics ASAP 2010 surface area and pore size analyzer. The sample for surface area analysis was activated by immersing as-synthesized **TIF-2** with methanol and then dichloromethane, followed by evacuation at room temperature. The activated sample was characterized by XRD to confirm that it has the same structure with as-synthesized sample (Figure S14, Supporting Information). The sample was degassed at 250 °C prior to the measurement. A type I isotherm was observed, indicating that **TIF-2** is microporous (Figure 5). The Langmuir surface area is 618.2 m^2/g using the data in the range of $P/P_0 = 0.065−0.208$. A single data point at relative pressure 0.208 gives a micropore volume of 0.206 cm^3/g by Horvath−Kawazoe equation. The median pore size of 14.1Å was also calculated.

Conclusions

Five 4-connected zeolitic metal imidazolate frameworks have been synthesized and structurally characterized. These materials exhibit four different 4-connected topologies. **TIF-2** possesses one-dimensional 12-ring channels, and its topology is not found in other 4-connected structures. It also exhibits permanent microporosity and has high thermal stability. **TIF-3** is the first known example of metal imidazolates with the zeolitic ACO topology. In **TIF-4**, **TIF-5Zn**, and **TIF-5Co**, two complementary ligands control the framework topology in a cooperative manner, which highlights the significance of framework building units (i.e., cross-linking ligands) in the control of the framework topology. This work also illustrates how a subtle change in the experimental conditions such as solvent ratio or ligand ratio can dramatically alter the framework structure. All these observations underline the rich synthetic and structural chemistry of metal-imidazolate-based porous frameworks.

Supporting Information Available: X-ray crystallographic data (CIF), PXRD pattern, and TGA spectra (PDF). This material is available free of charge via the Internet at http://pubs.acs.org.

CM802400F